J Fluoresc (2010) 20:197–202
DOI 10.1007/s10895-009-0538-z

ORIGINAL PAPER

Excited State Absorption Study in Hematoporphyrin IX

Leonardo De Boni · Carlos Toro · Florencio E. Hernandez

Received: 27 April 2009 / Accepted: 27 August 2009 / Published online: 16 September 2009

Abstract We present the study of the excited state absorption of Hematoporphyrin IX dissolved in dimethyl sulfoxide. All measurements were carried out using open aperture Z-scan and white-light continuum pump-probe with picosecond pulses to avoid triplet excited state absorption. Without the latter contribution, the results obtained with both techniques show a transition to a high singlet excited state. The vibronic progression of the Q-band is observed due to photobleaching of the ground state. In addition, we show that the excited state presents reverse saturable absorption for most of the spectral range studied. A long relaxation component of the first singlet excited state was evidenced with the pump-probe experiment. This result is in agreement with fluorescence lifetime and fluorescence quantum yield measurements. In order to elucidate the origin of the nonlinear effects, we used a three-level energy diagram to describe the principal singlet-singlet transitions.

Keywords Excited state absorption · Photodynamic therapy · Multiphoton absorption · Porphyrin

Introduction

The treatment and cure of malignant neoplasm, commonly known as cancer, remain nowadays as some of the major challenges for the scientific community. According to statistics reported by the World Health Organization [1] and the National Cancer Institute [2], this disease is accountable for a large percentage of the registered deaths worldwide and in US. This clearly suggests the necessity of finding affordable and efficient treatments to battle against this disease.

Among the variety of existing methodologies for cancer treatment, photodynamic therapy (PDT) has become one of the most attractive procedures, with large endorsement and standard protocols. PDT involves three basic steps in its action mechanism. First, a drug containing a photosensitizing agent (typically a porphyrin-based compound) is administered to the patient and the former is taken up by malign cells. Next, the tissue is exposed to well controlled doses of visible light which excites the photosensitizing molecules to the singlet excited state. After experiencing intersystem crossing (ISC) to the long lived triplet excited state, energy transfer occurs leading to the formation of highly cytotoxic singlet oxygen and/or free radicals. Finally, cell growth is inhibited by the action of these cytotoxic species resulting in cells death [3]. Several details regarding clinical conditions, selectivity, specificity, benefits and drawbacks of this technique have been reported elsewhere [4, 5]. An important limitation of this procedure arises from the fact that the penetration depth of typical radiation wavelengths employed for linear excitation is confined to the surface. In order to overcome this difficulty, multiphoton absorption processes have been proposed and successfully used in PDT [6–8]. Due to the nonlinear nature of the simultaneous absorption process of n-photons ($n \geq 2$), this approach offers the advantages of a much deeper penetration depth due to excitation in a region (infrared) that is less scattered and far from tissue absorption [9].

As mentioned above, the use of a photosensitizing agent represents the first key step in the action mechanism of PDT. In this context, porphyrin and phthalocyanine

L. De Boni · C. Toro · F. E. Hernandez
Department of Chemistry, University of Central Florida,
P.O. Box 162366, Orlando, FL 32816, USA

F. E. Hernandez (✉)
CREOL/The College of Optics and Photonics,
University of Central Florida,
P.O. Box 162366, Orlando, FL 32816, USA
e-mail: florenzi@mail.ucf.edu

derivatives are considered to be the archetype by excellence in the design of efficient photosensitizing agents for PDT applications [10, 11]. Schneckenburger et al. extensively studied, at the end of 1980 decade, the time-resolved fluorescence properties of these types of PDT agents [12, 13]. Therefore, it becomes necessary to study in detail the linear and nonlinear optical properties of these type of molecular systems, especially those related to the dynamic of the singlet and triplet excited states [14, 15].

In this article, we report the characterization of the singlet excited state dynamics of hematoporphyrin IX (HpIX), one of the components of Photofrin® II, the exclusive FDA approved drug for PDT. Studies were performed using picosecond nonlinear spectroscopy. During this excitation time regime, one can avoid the contribution of the triplet excited state, consequently, only absorption processes related to the singlet excited states can be considered. In order to obtain reliable experimental results and confirm the proposed model to describe the population dynamic in HpIX, we have performed nonlinear measurements using two different techniques as well as fluorescence lifetime.

Experimental

Hematoporphyrin IX dihydrochloride (inset Fig. 1) and dimethyl sulfoxide (DMSO) were purchased from Frontier Scientific and Sigma-Aldrich, respectively, and used as received. The linear absorption spectrum of HpIX dissolved in DMSO (see Fig. 1) at a concentration of *ca.* 1.7×10^{-4}M was collected with a single-beam spectrometer (Agilent 8453) using a 1-mm quartz cell (contribution from solvent and the cell was subtracted). The one photon fluorescence spectrum and fluorescence lifetime were obtained pumping the sample with the second harmonic beam (532 nm) coming out of a mode-locked Nd:YAG laser, 25-ps (FWHM), working at 10 Hz repetition rate. The signal was collected through a multimode optical fiber coupled to a spectrograph equipped with an ICCD camera as detector (Andor Shamrock sr-303i). A PTI Quanta Master spectrofluorimeter (model QM-3/2005) was used to measure the fluorescence quantum yield, ϕ_f, using the standard method [16] with rhodamine 6G in ethanol as reference (ϕ_{std}=0.95).

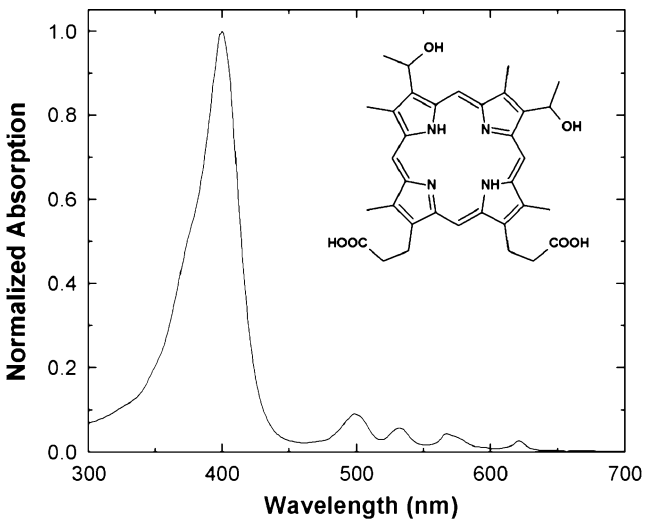

Fig. 1 Normalized linear absorption spectrum of HpIX in DMSO. Inset portraits the structure of HpIX

The excited state absorption dynamic of HpIX was studied using the well-known open aperture Z-scan [17] technique and white-light continuum (WLC) pump-probe [18]. The former was employed to perform measurements inside the linear absorption region using a tunable optical parametric generator (OPG) pumped by the third harmonic (355 nm) of the same laser utilized for fluorescence measurements. In order to obtain the Z-scan signatures, the sample was translated along the beam path (z-axis) across the focus of the laser beam. The transmitted light was fully collected with a convergent lens and focused into a silicon detector. The results, presented as the normalized transmittance, refer to the transmittance at different z positions (from $-z$ to $+z$) normalized to the one far from the focus (linear transmittance). On the other hand, when using the standard pump-probe setup, the probe beam (WLC) was attenuated to avoid significant excitation of the HpIX ground state. The pump beam energy (<1.5 μJ), however, was high enough to excite a great portion of molecules that were probed by the WLC beam as a function of the delay time. In order to verify that photodamage of the sample did not occur by the action of the pump beam, linear absorption measurements were carried out after each pump-probe experiment. For the pump beam, we used the OPG tuned at 530 nm to excite HpIX in the Q-band. In order to generate the WLC beam, the fundamental (1064 nm) from the pump laser was focused into a 10-cm cylindrical cell containing double distilled water. Approximately a 300 nm broadband spectrum in the visible region (450–750 nm) was produced [19]. After the cell, a band-pass filter and an achromatic lens were used to remove the fundamental and collimate the WLC beam, respectively. With the aim of achieving a stable and weak WLC, an iris was used to select the central portion of the WLC beam. Additional neutral density filters were employed to reduce the WLC intensity. An Ocean Optics USB 2000 system was used to collect the WLC beam after passing for a 1-mm quartz cell containing the sample. This system provided good resolution (~2 nm) and fast reading time. The zero delay time between pump and probe was found through a sum of frequencies process in a thin BBO crystal. Measurements of HpIX were carried out at a concentration of *ca.* 1.1×10^{-3}M.

Results and discussion

Figure 2 shows the fluorescence spectrum of HpIX/DMSO as a function of the gate delay time. This plot evidences two well defined bands centered at 630 and 700 nm. Both bands present the same fluorescence decay time, τ_f (approximately 17 ns), attributed to monomeric species of HpIX [20]. τ_f was obtained by adjusting the experimental data with a single exponential decay function. The inset illustrates the fit (solid line) for the peak centered at 630 nm. In addition, we also measured the fluorescence quantum yield for this compound, ϕ_f=0.08. The observed low ϕ_f, similar to that reported in porphyrin free-base [21], Zinc porphyrin [22] and indocyanine green [23], is a consequence of the dominating non-radiative relaxation processes, i.e. internal conversion (IC) and/or intersystem crossing (ISC). This result, in conjunction with the long fluorescence lifetime, suggests that molecules in the first excited state will experience a high ISC rate, thus increasing the triplet excited state population. With the aim of quantifying the rate of ISC (k_{ISC}), we used some approximations that have been proposed in the literature for the calculation of this parameter. First, one recognizes that the fluorescence lifetime (τ_f) accounts for the contribution from radiative (k_{rad}), internal conversion (k_{IC}) and intersystem crossing rates, i.e. $\tau_f = (k_{rad} + k_{IC} + k_{ISC})^{-1}$. Next, the ISC rate is calculated through $k_{ISC} = \phi_T/\tau_f$; where ϕ_T corresponds to the triplet excited state quantum yield. The intersystem crossing time can be easily estimated by $\tau_{ISC} = 1/k_{ISC}$. Therefore, in order to estimate the intersystem crossing rate the only requirement is to find reliable values of ϕ_T, which can actually be directly correlated to the singlet oxygen quantum yield (ϕ_Δ), according to reference [24].

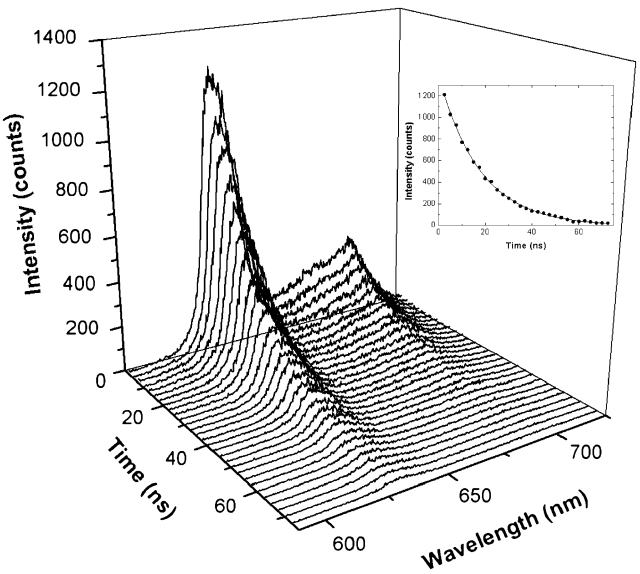

Fig. 2 Fluorescence spectra of HpIX in DMSO as a function of the gate delay time. Inset depicts the fluorescence decay at 630 nm (τ_f=17 ns)

Recently, Mathai et al. [25] reported experimental values of singlet oxygen quantum yield of HpIX in four different polar protic and aprotic solvents spanning from 0.5 to 0.85. These results are in agreement with values reported previously by different groups in similar systems [26–28]. Considering that DMSO is a polar solvent with a polarity function (Δf) similar to acetone, we used a value of ϕ_Δ=0.69 reported for HpIX in acetone as a reference [25]. Then, along with the approximation $\phi_\Delta \approx 0.79\phi_T$ reported in reference [29], we estimate an $\phi_T \approx 0.86$. Based on this value, one can estimate a $k_{ISC} \approx 5\times10^7 s^{-1}$, thus, $\tau_{ISC} \approx 20$ ns. Next, knowing that $k_{rad} = k_{ISC}(\phi_f/\phi_T)$ and $k_{IC} = (1/\tau_f) - k_{rad} - k_{ISC}$ [21], we proceeded to estimate both parameters. The values obtained are at least one order of magnitude less than the intersystem crossing rate. Therefore, it is expected that the radiative and internal conversion processes will take place in a much longer time scale (few hundred nanoseconds). This implies that ISC is the most likely radiationless pathway in HpIX. Additional studies confirm that related porphyrin-based photosensitizing agents posses a triplet excited state lifetime in the order of few hundred microseconds which guarantee the generation of cytotoxic species [21,30]. All these factors combined validate the certainty in using HpIX as a photosensitizing agent for PDT due to its ability to readily generate singlet oxygen.

Based on the fact that the laser presents a 25 ps pulse width, we considered only the transitions between three energy levels to explain the excited state absorption for HpIX. According to this model (inset Fig. 3), molecules in the ground state (S_0) can be excited to the first excited state, S_1 (Q-band), with a transition probability described by the ground state absorption cross-section, $\sigma_{01}(\lambda)$. Molecules in S_1 can then relax back to the ground state with a rate given by the relaxation time of the state, τ_{10}, or be promoted to another excited state, S_n, with a dependency expressed by the excited state absorption cross-section ($\sigma_{1n}(\lambda)$). Once in S_n, molecules decay back to the first singlet excited state during a time scale described by τ_{n1}. Considering only these processes, we were capable of theoretically reproduce the Z-scan signatures and then obtain, within a good approximation, the excited state absorption coefficient.

In order to develop a simplified set of rate equations to describe the population dynamic for the three-level energy diagram, we formulated some considerations related with the laser pulse and relaxation times of the states. First, according to the long fluorescence lifetime and the experimentally estimated energy of the highest occupied molecular orbital (HOMO) and lowest unoccupied molecular orbital (LUMO) band gap (~1.9 eV), which suggest low losses between the first and ground state due to internal conversion (~8–10%), we assumed that the population

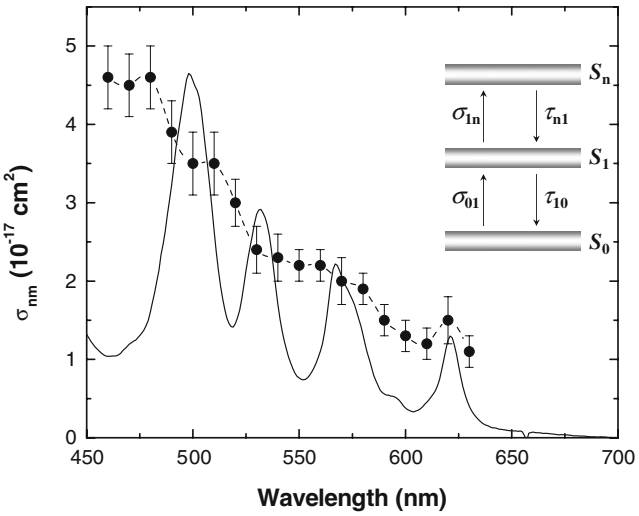

Fig. 3 Wavelength dependence of the absorption cross-section of HpIX in DMSO for the ground (solid line) and first excited (solid points) states, σ_{01} and σ_{1n}, respectively. Inset shows the three-level system used to obtain the values of σ_{1n}

promoted for the first excited state do not relax during the laser pulse time, τ_{pulse}, i.e. $\tau_{10} >> \tau_{pulse}$. Semiempirical calculations of the HOMO and LUMO support the previous statement. Details from these calculations will be addressed below. Second, we considered the relaxation time from S_n to S_1, τ_{n1}, to be much faster than τ_{pulse}. This statement is in agreement with values reported in the literature for porphyrin-based compounds [31–33], which relaxation times are in the scale of a few hundred femtoseconds. Consequently, using fast time and low pulse energy, we can consider a negligible accumulated population on S_n. This is equivalent to consider that the population of the first excited state is steady during the pulse. Taking into account these approximations, the rate equation to describe the populations is:

$$\frac{dn_0(t)}{dt} = -n_0(t)W_{01}(z,\lambda) + \frac{[1-n_0(t)]}{\tau_{10}}, \qquad (1)$$

where n_i are the population fraction of the singlet states (S_i) with $n_0(t) + n_1(t) + n_n(t) = 1$, *and* $1 - n_0(t) = n_1(t)$. $W_{01}(z,\lambda) = \sigma_{01}(\lambda)I(z)/h\nu$ is the transition rate for $S_0 \rightarrow S_1$. $I(z)$ is the excitation intensity at each z position, h is the Planck constant, and ν is the photon frequency. Solving Eq. 1 numerically we obtained the population dynamic of each state as well as a description of the temporal evolution of the absorption coefficient:

$$\alpha(t,\lambda) = N[n_0(t)\sigma_{01}(\lambda) + n_1(t)\sigma_{1n}(\lambda)]. \qquad (2)$$

Here, N is the number of molecules/cm^3. We should highlight that the only fitting parameter in Eq. 2 is $\sigma_{1n}(\lambda)$, because $\sigma_{01}(\lambda)$ is obtained through the linear absorption spectrum. Stimulated emission was initially considered in the description of the temporal evolution of the absorption coefficient. However, the contribution from this effect was found to be less than 1% and, it was omitted in the description of our three-level model.

As mentioned before, by fitting the normalized transmittance (Z-scan curves), we were able to describe the excited state cross-sections for HpIX over a broad spectral range (460 nm–630 nm). Figure 3 (closed circles) displays the measured excited state cross-section spectrum. The dashed line is only showed to guide the reader and it is not meant to be a fitting. From this plot, it is clear that, for most wavelengths, the absorption cross-section of the excited state is higher than that of the ground state, having a maximum of 5 folds around 460 nm. This trend in cross-sections, $\sigma_{1n}(\lambda) > \sigma_{01}(\lambda)$, is known as reverse saturable absorption (RSA). Nonetheless, for some other wavelengths, the values are close to the ground state. In these optical regions, the transition to the excited state does not change significantly the absorption of light. At 500 nm, HpIX presents an increase in the transmittance, describing a saturable absorption process. A similar behavior was observed for triplet-triplet dynamic studied by Gadonas and co-workers [34].

Semiempirical calculations were also performed using Hyperchem to estimate the energy of the frontier orbitals, HOMO and LUMO, of HpIX in gas phase. These orbitals are considered of particular interest because they may represent the main contribution to the electronic transitions. In this context, the structure of HpIX was first optimized by using semiempirical method AM1 [35]. Afterward, the electronic spectrum (excited states energies) was calculated using ZINDO/S [36]. This procedure allowed us to calculate an HOMO-LUMO band gap of 1.6 eV, which is relatively close to the experimental value (~1.9 eV). The observed differences could be attributed to the semiempirical nature of the method as well as the lack of solvent effects during the calculation. Figure 4 illustrates the spatial distribution of HOMO and LUMO for HpIX. Interestingly, both frontier orbitals evidence asymmetry in the charge

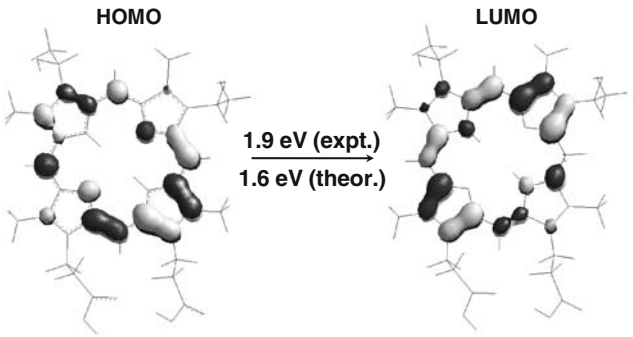

Fig. 4 Frontiers orbitals, HOMO and LUMO, of HpIX in gas phase calculated with the ZINDO/S method

distribution within the molecule. This feature is usually expected for push-pull systems that undergo intramolecular charge transfer from donor (-OH) to acceptor (-COOH) groups.

In order to confirm our previous analysis, we performed WLC pump-probe measurements to obtain the normalized transmittance (NT) spectrum as a function of time. Basically, this experiment provides information concerning the spectral regions in which the absorption of the sample increases or decreases as well as for how long the population stays in the excited states. During the total time delay employed in this experiment (roughly 270 ps), we observe that the NT kept constant for all the spectral range. This corroborates that the first excited state has a long lifetime, which agrees with the fluorescence lifetime. Yet, the second excited state lifetime cannot be quantified because our pulse width is much longer in time. Figure 5 portrays the NT (solid line) for a time delay (50 ps) at which the pump and probe beams are not overlapping. Additionally, the temporal profile for three selected wavelengths has been included (inset). At this time, all possible transitions induced by the pump beam are granted to have occurred and only transitions induced by the probe beam will take place. At this stage, a great portion of molecules are accumulated in the first singlet state, almost depleting the ground state. Based on this, we can consider that the probe beam will mostly probe the transition between $S_1 \rightarrow S_n$, and the changes in the transmittance are due to this excitation, starting at 700 nm, as well as the contribution from photobleaching of the Q-band. This feature has been previously observed in a gold porphyrin [37].

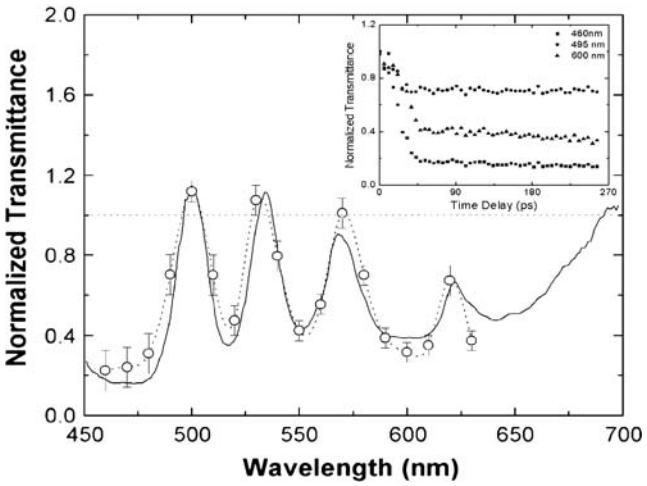

Fig. 5 Normalized transmittance for the HpIX/DMSO solution obtained using the white light continuum (WLC) pump-probe technique (solid line). The open circles represent the ratio between σ_{01} and σ_{1n}. The latter was obtained with Z-scan measurements. Inset shows typical normalized transmittance signal for three different wavelengths as a function of time delay

The analysis of the pump-probe NT confirms the Z-scan results. Essentially, the behavior of the NT matches with the behavior described by the excited state cross-section spectrum. According to the simulation of the Z-scan results using the rate equations, the population dynamics describes a high number of molecules in the first excited state. Based on this fact, we calculated the ratio between $\sigma_{01}(\lambda)$ and $\sigma_{1n}(\lambda)$ to construct the shape of the NT spectrum if a great number of molecules are excited (see open circles in Fig. 5). It can be observed that this curve follows the NT spectrum obtained with the pump-probe technique. This result suggests that the depletion of the ground state also occurs in the WLC pump-probe. In this case, both techniques converge for the same result, and using the better wavelength resolution of the WLC one can describe with more precision the behavior of the $\sigma_{1n}(\lambda)$. When the values of $\sigma_{01}(\lambda)$ and $\sigma_{1n}(\lambda)$ are close, for the same wavelength, it means that the normalized transmittance will be close to one. For example, taking three distinct wavelengths we can observe the convergence between both techniques. At 600 nm, the excited state cross-section is ~3.5 times higher than the ground state, which means that the NT will be less than one. Another wavelength of interest is around 540 nm, which value of NT approaches unity. However, at 500 nm, the increase of the normalized transmittance agrees with an excited state absorption cross-section value lower than that of the ground state. The pump-probe measurement, however, shows that the absorption between both excited states begins at 700 nm. This information is not revealed by Z-scan measurements because of the degeneracy of the technique. In other words, Z-scan cannot measure excited state absorption if the ground state absorption cross-section is null.

Conclusions

Using two different nonlinear optical techniques, namely Z-scan and white-light pump-probe, we were able to demonstrate that the excited state absorption cross-section of Hematoporphyrin IX in solution is greater than that of the ground state for most wavelengths in the visible range. In addition, white-light pump-probe results reveal that the excited state absorption begins at 700 nm. Besides, features of the Q-band, such as photobleaching, are observed with this technique. The quantification of fluorescence lifetime and fluorescence quantum yield, in combination with the excited state characterization, indicates that HpIX will favorably undergo intersystem crossing leading to a high generation of singlet oxygen. Therefore, it has been demonstrated that HpIX is indeed a potential good photosensitizing agent for photodynamic therapy.

References

1. Danaei G, Vander Hoorn S, Lopez AD, Murray CJ, Ezzati M (2005) Lancet 366:1784
2. Espey DK, Wu X, Swan J, Wiggins C, Jim MA, Ward E, Wingo PA, Howe HL, Ries LAG, Miller BA, Jemal A, Ahmed F, Cobb N, Kaur JS, Edwards BK (2007) Cancer 110:2119
3. Henderson BW, Dougherty TJ (1992) Photodynamic therapy. CRC, New York
4. Ackroyd R, Kelty C, Brown N, Reed M (2001) Photochem Photobiol 74:656
5. Brown SB, Brown EA, Walker I (2004) Lancet Oncol 5:497
6. Bhawalkar JD, Kumar ND, Zhao CF, Prasad PN (1997) J Clin Laser Med Surg 15:201
7. Hossain SMZ, Azam SMG, Babar SME (2006) Mol Cell Toxicol 2:1
8. Ogawa K, Kobuke Y (2008) Anti-cancer Agents Med Chem 8:269
9. Cohanoschi I, Echeverria L, Hernandez FE (2006) Chem Phys Lett 419:33
10. Bonnett R (1995) Chem Soc Rev 24:19
11. Sternberg ED, Dolphin D, Bruckner C (1998) Tetrahedron 54:4151
12. Schneckenburger H, Seidlitz HK, Ebertz J (1988) J Photochem Photobiol B 2:1
13. Schneckenburger H, Feyh J, Gotz A, Frenz M, Brendel W (1987) Photochem Photobiol 46:765
14. Shen L (2008) J Mol Struct Theochem 862:130
15. Zhang JZ, O'Neil RH, Evans JE (1994) Photochem Photobiol 60:301
16. Lakowicz J (1999) Principles of fluorescence spectroscopy. Kluwer Academic, New York
17. Sheik-Bahae M, Said AA, Wei T, Hagan DJ, Van Stryland EW (1990) IEEE J Quant Electron 26:760
18. Negres RA, Hales JM, Kobyakov A, Hagan DJ, Van Stryland EW (2002) Opt Lett 27:270
19. De Boni L, Toro C, Hernandez FE (2008) Opt Express 16:957
20. Andersson-Engels S, af Klinteberg C, Svanberg K, Svanberg S (1997) Phys Med Biol 42:815
21. Goncalves PJ, Aggarwal LPF, Marquezin CA, Ito AS, De Boni L, Neto NMB, Rodrigues JJ, Zilio SC, Borissevitch IE (2006) J Photochem Photobiol A Chem 181:378
22. Goncalves PJ, De Boni L, Borissevitch IE, Zilio SC (2008) J Phys Chem A 112:6522
23. De Boni L, Rezende DCJ, Mendonca CR (2007) J Photochem Photobiol A Chem 190:41
24. Byeon CC, McKerns MM, Sun W, Nordlund TM, Lawson CM, Gray GM (2004) Appl Phys Lett 84:5174
25. Mathai S, Smith TA, Ghiggino KP (2007) Photochem Photobiol Sci 6:995–1002
26. Tanielian C, Heinrich G (1995) Photochem Photobiol 61:131
27. Echeverria L, Rodriguez L, Marcano A, Estrada O, Salazar M, Quintero F (2005) Proc. SPIE 6009, 60090 K
28. Nielsen CB, Forster JS, Ogilby PR, Nielsen SB (2005) J Phys Chem A 109:3875
29. Aggarwal LPF, Baptista MS, Borissevitch IE (2007) J Photochem Photobiol A Chem 186:187
30. Molnar A, Dedic R, Korinek M, Svoboda A, Hala J (2005) J Mol Struct 744–747:723
31. Mataga N, Shibata Y, Chosrowjan H, Yoshida N, Osuka A (2000) J Phys Chem B 104:4001
32. Gurzadyan GG, Tran-Thi T-H, Gustavsson T (1998) J Chem Phys 108:385
33. Enescu M, Steenkeste K, Tfibel F, Fontaine-Aupart M-P (2002) Phys Chem Chem Phys 4:6092
34. Gadonas R, Kapociute R, Krasauskas V, Piskarskas A, Rotomskis R (1986) Chem Phys Lett 129:603
35. Dewar MJS, Zoebisch EG, Healy EF, Stewart JJP (1985) J Am Chem Soc 107:3902
36. Ridley J, Zerner M (1973) Theor Chim Acta 32:111
37. Andreasson J, Kodis G, Lin S, Moore AL, Moore TA, Gust D, Martensson J, Albinsson B (2002) Photochem Photobiol 76:47